The Role of Degeneracy

In this handout, we'll consider how the outcome of stellar evolution — whether we end up with a white dwarf or a supernova — depends on the initial mass of the star. If electron degeneracy did not occur, then all stars would be able to burn their way through to ^{56}Fe (see *Handout* XXVIII). In reality, of course, the onset of degeneracy in a stellar core prevents it from contracting and heating up. Unless further mass is added to the core[1] , it will never reach the temperature required to ignite the next fuel in the burning sequence; instead, it will cool down as the star transitions into a white dwarf.

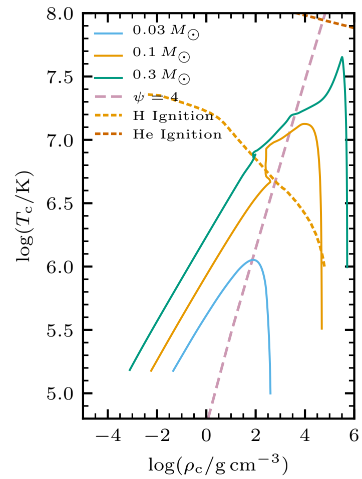

Figure 1: Paths followed in the $\log\rho_c$–$\log T_c$ plane for *MESA* models with initial masses $M/M_\odot = (0.03, 0.1, 0.3)$, from the pre-main sequence to the final states. The diagonal dashed line divides the plane approximately into ideal-gas (left) and degenerate (right) regimes, while the dotted lines show the ignition thresholds for hydrogen and helium.

The Hydrogen Burners

Fig. 1 plots the paths followed by three very low-mass *MESA* models in the $\log\rho_c$–$\log T_c$ plane, as they evolve from the pre-main sequence phase through to their final states. The cores of all three models begin at low temperature and density in the ideal-gas regime. With Kelvin-Helmholtz contraction, the models' central temperatures initially increase according to the formula derived in *Handout* IX:

$$\log T_c \approx \frac{1}{3}\log\rho_c + \frac{2}{3}\log M + C$$

(eqn. 4, *ibid.*). However, owing to its lower temperature at a given density, the $0.03\,M_\odot$ model passes into the degenerate-electron regime before it can reach the threshold $\log T_c \approx 7$ for hydrogen ignition. Therefore, this model corresponds to a brown dwarf rather than a star — as do all sub-stellar objects with initial masses $M \lesssim 0.08\,\mathrm{M}_\odot$.

The other two models successfully ignite hydrogen in their cores; but after the hydrogen is exhausted they, too, develop degenerate cores. For a while, the addition of helium to the core (by the hydrogen-burning shell around it) allows their central temperatures to continue to climb. Before they can reach the threshold $\log T_c \approx 8$ for helium ignition, however, the shell runs out of further hydrogen to consume; the stars instead cool down to form helium white dwarfs. The same fate befalls all stars with initial masses in the interval $0.08\,\mathrm{M}_\odot \lesssim M \lesssim 0.7\,\mathrm{M}_\odot$.

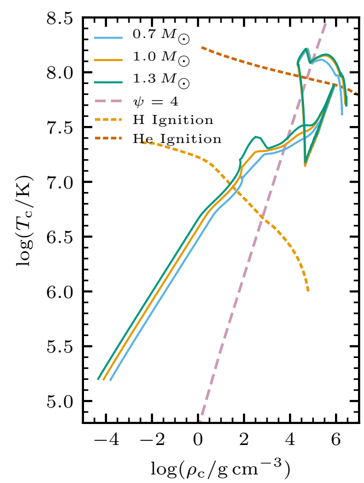

Figure 2: As in Fig. 1, except that *MESA* models with initial masses $M/M_\odot = (0.7, 1.0, 1.3)$ are shown.

The Helium Burners

Fig. 2 repeats Fig. 1, but now for three low-mass *MESA* models (including a solar-mass model). The cores of these models also become degenerate after hydrogen burning. However, in contrast to the very low mass models, they are able to add sufficient mass to their cores

[1] The addition of mass to a degenerate core heats it *indirectly*, by raising the gravity and therefore temperature in the burning shell surrounding the core. *Handout* XXII demonstrates this mechanism for degenerate helium cores on the RGB.

during hydrogen shell burning that they reach the helium ignition threshold. Because ignition occurs under degenerate conditions, all three models pass through a helium flash. The effect of the initial flash and the subsequent after-flashes (see *Handout* XXIII) is to expand the core and thereby reduce the central density. During this process, the central temperature initially drops, but then it increases again, creating a characteristic 'V' shape in the $\log \rho_c$–$\log T_c$ diagram. After the flashes have subsided, the center is back in the ideal-gas regime, where it remains for the duration of core helium burning.

After the end of core helium burning, as the models climb the AGB, their carbon-oxygen cores soon re-enter the degenerate regime. Significant mass-loss on the AGB prevents them from adding much further mass to these cores; therefore, they never reach the carbon ignition threshold $\log T_c \approx 8.7$, instead cooling down to form carbon-oxygen white dwarfs.

Fig. 3 shows the case for three intermediate-mass *MESA* models. Like the low-mass models, the $M = 2\,M_\odot$ case undergoes a helium flash. However, the $M = 3\,M_\odot$ and $M = 7\,M_\odot$ models ignite helium while the core is still in the ideal-gas regime, and don't experience a flash. In all three cases, the core becomes degenerate after helium burning is complete; failing to ignite carbon, they also become carbon-oxygen white dwarfs. The same fate befalls all stars with initial masses $0.7\,M_\odot \lesssim M \lesssim 8\,M_\odot$; within this interval, $M \approx 2.1\,M_\odot$ is the dividing line between the low-mass stars that experience a helium flash, and the intermediate-mass stars that don't.

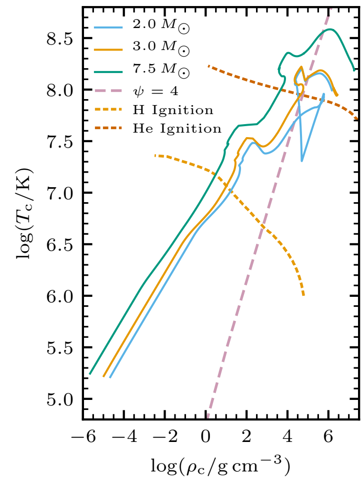

Figure 3: As in Fig. 1, except that *MESA* models with initial masses $M/M_\odot = (2.0, 3.0, 7.0)$ are shown.

The Carbon (& Beyond) Burners

Fig. 4 repeats Fig. 1, but now for a pair of high-mass *MESA* models. After core hydrogen and helium burning, both models reach sufficiently high central temperatures for carbon burning to occur. For the $16\,M_\odot$ model the steady addition of mass to the core causes the central temperature to continue climbing, even when the core becomes somewhat degenerate. Hence, this model is able to proceed through the later burning stages until it forms a ^{56}Fe core and collapses. This outcome is shared by stars with initial masses $M \gtrsim 11\,M_\odot$.

The $10\,M_\odot$ model lacks sufficient envelope mass to keep feeding the core after carbon burning has completed. Instead, it cools down as an oxygen-neon white dwarf — a fate common to stars with masses in the (very approximate interval) $8\,M_\odot \lesssim M \lesssim 11\,M_\odot$.

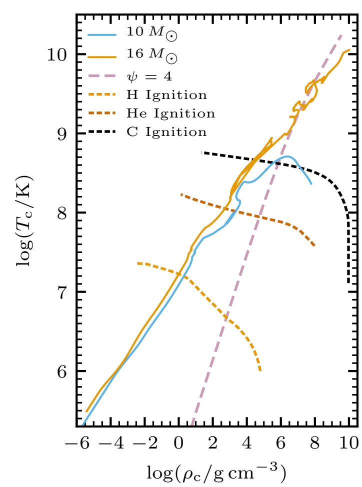

Figure 4: As in Fig. 1, except that *MESA* models with initial masses $M/M_\odot = (10, 16)$ are shown, along with an additional ignition line for carbon.

Further Reading

Kippenhahn, Weigert & Weiss, §§34.8,35.2